

# Electrocatalysis via Intrinsic Surface Quinones Mediating Electron Transfer to and from Carbon Electrodes

Danlei Li, Christopher Batchelor-McAuley, Lifu Chen, Richard G. Compton\*

Department of Chemistry, Physical and Theoretical Chemistry Laboratory, University of Oxford, South Parks Road, Oxford OX1 3QZ

\*Corresponding author:

Email: Richard Compton [Richard.compton@chem.ox.ac.uk](mailto:Richard.compton@chem.ox.ac.uk)

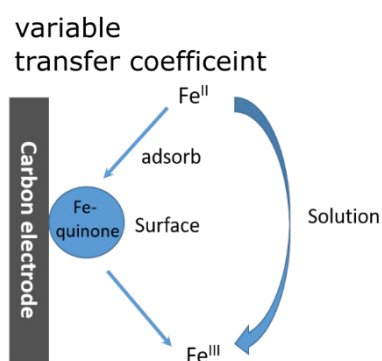
Phone: +44(0) 1865 275957

Fax: +44(0) 1865 275410

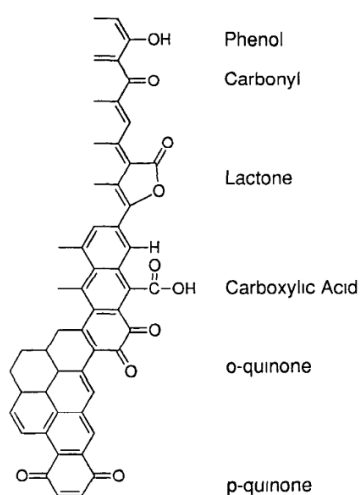
## Abstract

The electrochemistry of the  $\text{Fe}^{2+}/\text{Fe}^{3+}$  redox couple in aqueous solution at carbon electrodes is shown to be catalysed by surface quinone groups intrinsically present in the carbon surface. Such mediation is long speculated but hitherto unproven.

## TOC Graphics



Low cost and abundant availability encourage carbon based electrodes to be widely used throughout electrochemical technologies including in fuel cells, batteries, sensors, etc.<sup>1-3</sup> Nevertheless understanding electron transfer at the carbon electrode-electrolyte interface is challenging over and above that at metal electrodes, such as gold or platinum, partly because carbon electrodes come in many forms – graphite, (doped) diamond, nanotubes, graphene, carbon black, glassy carbon, ... - and partly because the carbon surface is particularly chemically reactive. Thus it has long been recognised, largely as a result of the pioneering work of McCreery<sup>4-6</sup>, that a wide diversity of functional groups may exist on carbon surfaces as shown schematically in Scheme 1<sup>7</sup>, including quinones which derive from the reaction of molecular oxygen or water with the surface<sup>8</sup>. Of the many groups shown, the quinones have excited particular interest since as isolated molecules they are electroactive in both aqueous and non-aqueous solutions. This, in the case of intrinsic surface species, has been exploited, for example, in the development of carbon based pH sensors where voltammetric signals due to the two electron, two proton reduction of quinones are used to indicate the pH of aqueous solutions<sup>9-10</sup>. Voltammetric signals from surface quinones have been seen on a variety of carbon surfaces and their near ubiquity raises the possibility of electron transfer to solution phase redox couples at carbon electrodes being mediated via electron transfer to or from the intrinsic surface quinone groups present. Such ideas are supported by reports of carbon electrodes deliberately modified by quinone groups, via covalent attachment, adsorption or immobilisation of polymers, which have been shown to electrocatalyse, via mediation, the reduction of, for example, peroxidase<sup>11</sup>, oxygen<sup>12-13</sup>, quinones<sup>14</sup> and the oxidation of several bioanalytes<sup>15</sup>. Further it has been suggested that electron transfer via intrinsic surface quinones is responsible for increased oxygen reduction activity<sup>16</sup> and for other electrochemical processes<sup>17</sup>.



*Scheme 1 Representation of various functional groups on Carbon surfaces. The picture was adapted from ref.<sup>7</sup>*

The aim of this paper is to identify an electrochemical reaction in which intrinsic surface quinones unambiguously mediate and catalyse electron transfer. In particular, we focus on the  $\text{Fe}^{2+}/\text{Fe}^{3+}$  redox couple in aqueous acidic solution noting that  $\text{Fe(III)/quinone}$  mediated electron transfer is well documented in homogeneous conditions<sup>18-21</sup> for several biological systems. The  $\text{Fe}^{2+}/\text{Fe}^{3+}$  redox couple has also been applied in large-scale energy storage technologies such as redox flow batteries due to low cost, high abundant and low chemical toxicity<sup>22-23</sup>. Accordingly the  $\text{Fe}^{2+}/\text{Fe}^{3+}$  system in the form of ca. millimolar concentrations of  $\text{NH}_4\text{Fe}(\text{SO}_4)_2$  and  $(\text{NH}_4)_2\text{Fe}(\text{SO}_4)_2$  in 0.2 M  $\text{HClO}_4$  was investigated.

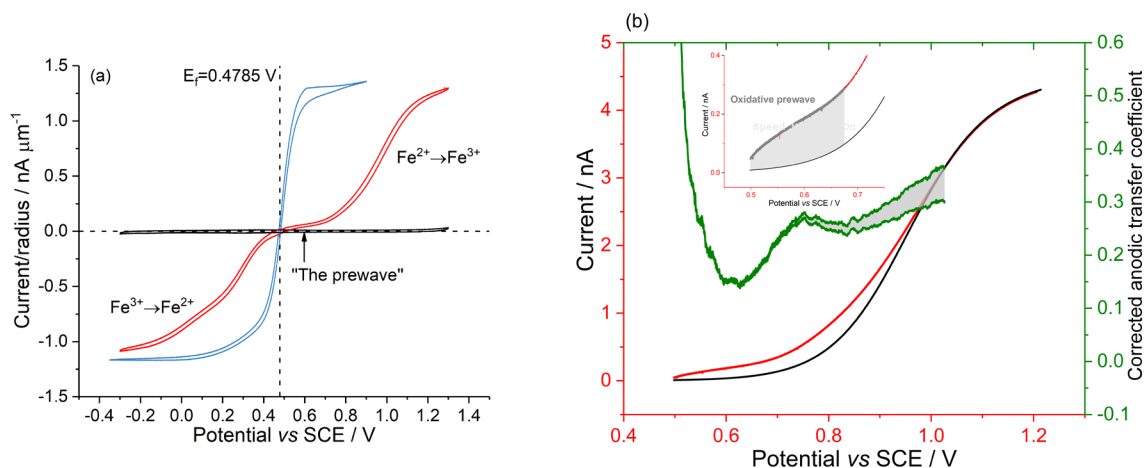


Figure 1 (a) Comparison of voltammograms normalised to electrode radius on a carbon microdisc electrode (radius=3.5  $\mu\text{m}$ ) (red) and a gold microdisc electrode (radius=5.15  $\mu\text{m}$ ) (blue) at 25 °C at 0.01  $\text{V s}^{-1}$  in a solution of  $\text{Fe}^{2+/3+}$  (5.0 mM  $(\text{NH}_4)_2\text{Fe}(\text{SO}_4)_2$ , 5.0 mM  $\text{NH}_4\text{Fe}(\text{SO}_4)_2$ , 2.5 mM  $(\text{NH}_4)_2\text{SO}_4$  with 0.2 M  $\text{HClO}_4$ ). The black curve represents the voltammetric response without  $\text{Fe}^{2+/3+}$  redox couple. The formal potential of the  $\text{Fe}^{2+/3+}$  redox couple is labelled as a vertical dashed line. The horizontal dashed line labels zero current. (b) Mass transport corrected anodic transfer coefficient plots with (green) and without (black) non-uniformly accessibility correction on the carbon microdisc electrode. The experimental oxidative voltammogram is shown as red curve and the black curve shows the simulated voltammogram on a microdisc electrode with an anodic transfer coefficient of 0.35. The current range is 1%-95% of the true steady-state current. The inset represents the zoomed-in version of the oxidative pre-wave (highlighted in grey).

**Voltammetric response on gold and carbon microdisc electrodes** Fig 1(a) depicts the voltammetric response of a gold micro-electrode (blue-line) in a solution containing both  $\text{Fe}^{2+}$  and  $\text{Fe}^{3+}$  (5 mM). On the gold electrode the redox process is, at low potentials, fully reversible as evidenced by the continuity in the voltammogram near the equilibrium potential where significant anodic and cathodic currents flow either side of the equilibrium potential. From this voltammetric response it is possible to determine the formal potential for the redox process ( $E_f^\ominus = 0.4785 (\pm 0.0006)$  V vs. SCE, which is different from the standard potential<sup>24</sup>) and the diffusion coefficients for the reduced and oxidised species,  $6.7 (\pm 0.1) \times 10^{-6}$  and  $5.5 (\pm 0.1) \times 10^{-6} \text{ cm}^2 \text{ s}^{-1}$  respectively (see SI sections 1 and 2). In contrast to the gold electrode the voltammetric response of the  $\text{Fe}^{2+/3+}$  redox couple is markedly slower on a carbon substrate. Overlaid on Fig 1(a) is the voltammetric response of a carbon microdisc electrode

under the same experimental conditions (red-line); the separation of the main waves indicating slower electron transfer. Moreover in the low anodic current region (0.5-0.7 V) the current is appreciably above zero before the main oxidative wave appears at a half-wave potential of 0.9483 V vs SCE. The half-wave potential for the oxidation process ( $\eta_{1/2} = +0.470$  V) has been shifted to a relatively higher overpotential as compared to the reduction ( $\eta_{1/2} = -0.258$  V), evidencing a distinct asymmetry in the nature of the electron transfer kinetics. On the reductive scan of the iron redox couple a clear inflection in the voltammogram is present; however, the voltammetry does not easily allow this process to be more clearly delineated, limiting mechanistic interpretation. Hence, the focus of this work is the origin of this non-zero current at low *anodic* overpotentials; the presence of this anodic pre-wave will be both fully evidenced and a surface quinone based explanation for its origin will be provided.

**Tafel analysis on the voltammogram at a carbon microdisc electrode** Tafel analysis provides a direct route by which transfer coefficient for a redox reaction can be determined. The transfer coefficient<sup>25-26</sup> is an experimentally measurable quantity and is related to the fraction (and hence asymmetry) of the electrostatic potential available for the oxidation or reduction process. Importantly, in the case of inner-sphere redox reactions this fraction of the electrochemical potential available for the redox process can be influenced by the electrodes double layer.<sup>27</sup> The anodic transfer coefficient ( $\alpha_a$ ) is defined as:

$$\alpha_a = \left( \frac{RT}{F} \right) \left( \frac{d \ln j_a}{dE} \right) \quad (1)$$

where R is the gas constant (8.314 J mol<sup>-1</sup> K<sup>-1</sup>), T is the temperature in K, F is the Faraday constant (96,485 C mol<sup>-1</sup>) and the anodic current density  $j_a$  has been corrected to account for changes in the concentration of the reactant at the electrode surface. For a carbon microdisc electrode although at low scan rates a steady-state mass-transport regime can be attained, the electrode surface is non-uniformly accessible. This non-uniformity means that, in contrast to other electrode geometries such as a hemispherical electrode, there is no exact analytical expression available to correct for the influence of the mass-transport conditions on the voltammetric response; consequently, the correction made in this work to extract the transfer coefficient is strictly only approximate (see SI section 3 for more details). Fig 1(b) depicts the anodic mass-transport corrected transfer coefficient for the oxidation of Fe<sup>2+</sup>, the grey area represents the estimated uncertainty in the mass-transport correction. Moreover, due to the limitations of the used methodology currents above 70% of the diffusion limited flux have not been considered for analysis. The measured transfer coefficient for this system is significantly below 0.5, where for a one electron process a value close to 0.5 is often observed for a redox outer sphere process. This experimental data evidences that the transfer

coefficient is not constant and varies as a function of the electrode potential. At higher over potentials ( $>1.0$  V) the transfer coefficient tends towards a value of 0.35 but at low over potentials the transfer coefficient is found to be significantly below this limit. Overlaid with the experimental voltammogram in Fig 1(b) is the simulated voltammetric response (black-line) for a simple one-electron transfer process with a symmetry factor of 0.35. Here for the simulation the standard electrochemical rate constant has been used as a fitting parameter and has a value of  $6 \times 10^{-7} \text{ m s}^{-1}$ . First, as anticipated from the measured transfer coefficient, at high overpotentials and near the mass-transport limit ( $>60\%$  of  $I_{s,s}$ ) the voltammetric response is well described by this simple single mechanistic pathway simulation model as shown in Fig 1(b). SI section 4 further investigates the ‘fitting’ of this simple one-electron simulation to the experimental data, further corroborating the conclusion that the transfer coefficient varies as a function of the applied electrode potential, no fixed value of the transfer coefficient is able to fit the experimental current across the full range of potentials.

The measured change in the transfer coefficient as a function of the applied potential is first strongly indicative of a change in the electrochemical redox mechanism. Second, as evidenced through comparison of the simulated and experimental data, at low overpotentials there is more current passed than would be expected for a simple mechanistic process. For this electrode geometry this pre-wave contributes approximately 0.2 nA of current and for clarity has been highlighted in the inlay of Fig 1(b). Moreover, for other electrode geometries where the mass-transport regime is less efficient this pre-wave becomes relatively larger. This latter point is evidenced in the SI section 5 through the study of the voltammetric response of a carbon fibre electrode under comparable experimental conditions; here the pre-wave is appreciably relatively larger on the microcylinder electrode. SI section 5.2 shows that the pre-wave current varies linearly as a function of  $\text{Fe}^{2+}$  concentration in the range of 5 to 20 mM, which is most likely due to the change in the surface coverage of the adsorbed species.

**Adsorption of  $\text{Fe}^{2+}/\text{Fe}^{3+}$  on a carbon microdisc electrode** We next turn to consider the physico-chemical origins of the observed pre-wave. Although the  $\text{Fe}^{2+/3+}$  redox couple is known to be sensitive to oxygen-containing functional groups on the electrode surface<sup>4-5</sup>, it has not been proved which specific functional groups are responsible for the catalysed reaction. The origin of the interaction between Fe ions and the functional groups which results in the occurrence of pre-wave was investigated. Transfer experiments were consequently conducted to study such potential adsorption behaviour. A carbon microdisc was immersed into a solution containing 2.5 mM  $\text{NH}_4\text{Fe}(\text{SO}_4)_2$  in 0.2 M  $\text{HClO}_4$ , and the voltammetric response of this interface studied before and after exposure to the solution. The voltammetric experiments were measured in the absence of Fe(III) in the solution phase; detailed procedures are provided in the Experimental Section. Fig 2(a) depicts examples of the measured voltammetric response of the electrode before (red-line) and after (black-line) immersion

in the iron containing solution. Voltammograms obtained in other solutions containing variable concentrations of  $\text{Fe}^{3+}$  can be found in SI section 6. For the clean carbon surface the voltammetric response of the electrode exhibits a relatively large capacitive charging current and at a pH of 0.69, a broad surface bound feature corresponding to the redox chemistry of surface quinone groups (at ca. 0.38 V vs SCE)<sup>9</sup>. From this voltammetric peak the surface coverage of catechol on a clean carbon electrode was calculated to be  $(4.33 \pm 0.66) \times 10^{-11} \text{ mol cm}^{-2}$  as ascertained from the integration of the quinone/catechol peak observed in blank solution. This value is consistent with the literature values for that of ortho-quinones measured on basal plane and edge plane pyrolytic graphite electrodes of  $1.7 \times 10^{-10}$  and  $2.0 \times 10^{-12} \text{ mol cm}^{-2}$ , respectively<sup>28</sup>. After, exposure of the electrode to the  $\text{Fe}(\text{II})$  containing solution an additional redox signal is observed at ca. 0.54 V vs SCE, the presence of this additional redox feature can be more fully resolved by background subtraction. Furthermore, the magnitude of this additional peak is not sensitive to the length of time (for times greater than ca. 2 minutes) the carbon electrode has been exposed to the iron solution. Fig 2(b) shows the voltammetric response of the iron exposed electrode after removal of the capacitive and quinone responses, where variable iron concentrations have been used. The voltammograms give well-defined surface-bound peaks at around 0.5 V in all cases; the peak charge increases with the increasing  $\text{Fe}^{3+}$  concentration in the range of 5 mM to 20 mM and becomes essentially constant when the  $\text{Fe}^{3+}$  concentration is larger than 20 mM. First, the charge passed oxidatively and reductively is comparable indicating that both the oxidised and reduced iron species adsorbed to the electrode surface. Second, the mid-point potential for the voltammetric feature is only shifted by less than 10 mV from the measured solution phase formal potential for the redox couple, indicating that the binding strength of both the oxidised and reduced species is very comparable. Third, integration of the peak enables the surface coverage of the adsorbed iron to be assessed as depicted in the inlay in Fig 2 which presents the measured  $\text{Fe}^{3+}$  adsorption isotherm on the carbon microdisc electrode in solutions containing variable concentrations of  $\text{Fe}^{3+}$ . The experimentally measured maximum surface coverage of adsorbed  $\text{Fe}^{3+}$  was calculated to be  $(4.42 \pm 0.18) \times 10^{-11} \text{ mol cm}^{-2}$ , which is very comparable to that expected from surface quinones. The consistency between the surface coverages of quinone/catechol and the Fe ions strongly indicates that the occurrence of the additional peaks is attributed to  $\text{Fe}^{2+/3+}$  adsorption on the electrode which mediates  $\text{Fe}^{2+}$  oxidation. Although it is possible that iron adsorption occurs via binding to other surface oxygen functionalities such as carboxylic acid groups, these alternate functionalities would need to have an identical surface coverage to the quinone. Furthermore, the binding of iron to catechol functionalities is well documented in the literature in contexts outside of electrochemistry<sup>29-30</sup>. Similar results were obtained for  $\text{Fe}^{2+}$  adsorption on carbon

electrodes, as provided in SI Section 7, which further proves both  $\text{Fe}^{2+}/\text{Fe}^{3+}$  redox couple is sensitive to the presence of quinone/catechol groups.

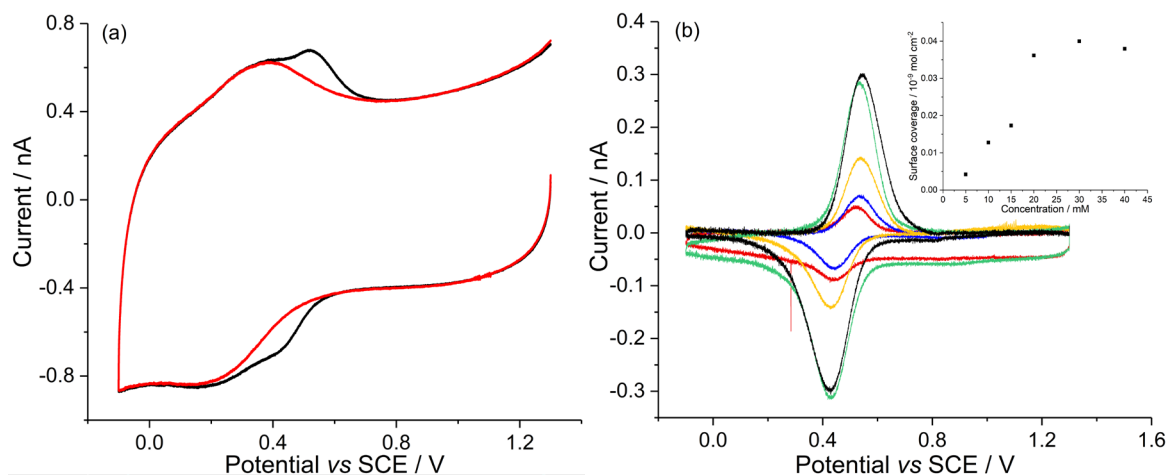
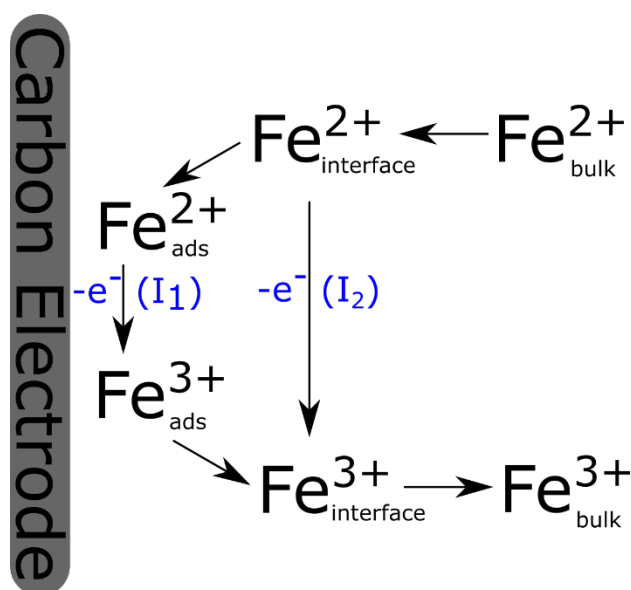


Figure 2 (a) Voltammograms of a carbon microdisc electrode ( $r=3.5 \mu\text{m}$ ) in blank solution before (red) and after (black) immersion in the iron containing solution. Blank solution composition: 2.5 mM  $(\text{NH}_4)_2\text{SO}_4$  with 0.2 M  $\text{HClO}_4$ . Iron containing solution: 15 mM  $\text{NH}_4\text{Fe}(\text{SO}_4)_2$ , 2.5 mM  $(\text{NH}_4)_2\text{SO}_4$  with 0.2 M  $\text{HClO}_4$ . (b) Voltammograms with background subtraction as a function of the concentration of  $\text{Fe}^{3+}$  (5 mM – red, 10 mM – blue, 15 mM – yellow, 20 mM – green and 30 mM – black) at 25 °C. The inset presents  $\text{Fe}^{3+}$  adsorption isotherm at 0.2 V  $\text{s}^{-1}$ .

The pre-wave observed on the carbon electrode in Fig 1 gives a quasi-steady-state-like behaviour. Such steady-state behaviour was also observed by Sato *et al.* in the investigation of the catalysis of the oxidation of  $\text{Fe}^{2+}$  in aqueous solution by  $[\text{Mo}(\text{CN})_8]^{3-}$  on a rotating disk pyrolytic graphite electrode<sup>31</sup>. On the basis of the above experimental results we propose that the  $\text{Fe}^{2+}$  oxidation on the carbon electrode can be understood via a mechanistic model involving two parallel pathways (Scheme 2). First, at low overpotentials there is a surface mediated redox reaction where the results are consistent with the oxidation proceeding via a surface adsorbed iron-quinone complex (pathway 1) and the current obtained from pathway 1 is labelled as  $I_1$ . Second, at higher overpotentials the oxidation proceeds via a direct solution phase oxidative route (Pathway 2) and the obtained current from this pathway is  $I_2$ . Here, for pathway  $I_1$  the likely rate determining step will be the desorption of the  $\text{Fe}^{3+}$  species. However, it should however be noted that an alternative reaction scheme whereby the surface adsorbed iron species serves to mediate the electron transfer in a manner comparable to that found for the self catalysis of catechol cannot be ruled out. However, it is more challenging to conceive of how such a mechanism could lead to the occurrence of two parallel electron transfer pathways, as experimentally evidenced by the measured transfer coefficient over a range of potentials. The transfer coefficient for this direct oxidative pathway ( $I_2$ ) has a value of approximately 0.35, as determined from the experimental data at high overpotentials whilst the value is much smaller at low overpotentials as presented in Figure 1(b). The switch in the electrode mechanism is reflected in the

measured transfer coefficient which is sensitive to the applied electrode potential. In the SI section 8 a detailed discussion and demonstration on this numerical model and how the presence of a parallel mechanism can cause such a change in systems transfer coefficient were provided.



*Scheme 2 Proposed two parallel pathways during the  $\text{Fe}^{2+}/3^+$  redox process in solution.*

To conclude, the surface quinones on carbon electrodes were found to intrinsically catalyse  $\text{Fe}^{2+}$  oxidation via the formation of Fe-quinone complexes under acidic conditions, which has long been observed but not proved. This quinone mediated redox process was observed as a quasi-steady-state like 'prewave' on a carbon microdisc electrode. Moreover, the presence of this electrocatalytic process (i.e. the pre-wave) is more apparent under lower mass-transport conditions and will likely be the dominant redox pathway when larger macroscale electrodes are used, as may be employed for example in a redox flow-cell battery.

## Acknowledgements

Danlei Li thanks the China Scholarship Council and University of Oxford for supporting her DPhil.

## Conflict of interest

There are no conflicts to declare.

**Supporting Information Available:** <determination of diffusion coefficients and the formal potential of the  $\text{Fe}^{2+}/3^+$  redox couple; the analysis of transfer coefficient; proposed mechanism model; experimental section>



## References:

1. Yue, L.; Li, W.; Sun, F.; Zhao, L.; Xing, L. Highly hydroxylated carbon fibres as electrode materials of all-vanadium redox flow battery. *Carbon* **2010**, *48* (11), 3079-3090.
2. Jiang, L.-C.; Zhang, W.-D. A highly sensitive nonenzymatic glucose sensor based on CuO nanoparticles-modified carbon nanotube electrode. *Biosensors and Bioelectronics* **2010**, *25* (6), 1402-1407.
3. Zhang, Y.; Liu, L.; Van der Bruggen, B.; Yang, F. Nanocarbon based composite electrodes and their application in microbial fuel cells. *Journal of Materials Chemistry A* **2017**, *5* (25), 12673-12698.
4. Chen, P.; Fryling, M. A.; McCreery, R. L. Electron transfer kinetics at modified carbon electrode surfaces: the role of specific surface sites. *Analytical Chemistry* **1995**, *67* (18), 3115-3122.
5. Chen, P.; McCreery, R. L. Control of electron transfer kinetics at glassy carbon electrodes by specific surface modification. *Analytical Chemistry* **1996**, *68* (22), 3958-3965.
6. McCreery, R. L. Advanced carbon electrode materials for molecular electrochemistry. *Chemical reviews* **2008**, *108* (7), 2646-2687.
7. Bard, A. J. *Electroanalytical Chemistry: A Series of Advances*. Taylor & Francis: 1990.
8. Chaisiwamongkhol, K.; Batchelor - McAuley, C.; Palgrave, R. G.; Compton, R. G. Singlet oxygen and the origin of oxygen functionalities on the surface of carbon electrodes. *Angewandte Chemie* **2018**, *130* (21), 6378-6381.
9. Chaisiwamongkhol, K.; Batchelor-McAuley, C.; Compton, R. G. Amperometric micro pH measurements in oxygenated saliva. *Analyst* **2017**, *142* (15), 2828-2835.
10. Lu, M.; Compton, R. G. Voltammetric pH sensor based on an edge plane pyrolytic graphite electrode. *Analyst* **2014**, *139* (10), 2397-2403.
11. Hoogvliet, J. C.; Van Os, P.; Van der Mark, E. J.; Van Bennekom, W. P. Modification of glassy carbon electrode surfaces with mediators and bridge molecules. *Biosensors and Bioelectronics* **1991**, *6* (5), 413-423.
12. Sarapuu, A.; Helstein, K.; Schiffrin, D. J.; Tammeveski, K. Kinetics of oxygen reduction on quinone-modified HOPG and BDD electrodes in alkaline solution. *Electrochemical and Solid State Letters* **2004**, *8* (2), E30.
13. Tammeveski, K.; Kontturi, K.; Nichols, R. J.; Potter, R. J.; Schiffrin, D. J. Surface redox catalysis for O<sub>2</sub> reduction on quinone-modified glassy carbon electrodes. *Journal of Electroanalytical Chemistry* **2001**, *515* (1-2), 101-112.
14. DuVall, S. H.; McCreery, R. L. Self-catalysis by catechols and quinones during heterogeneous electron transfer at carbon electrodes. *Journal of the American Chemical Society* **2000**, *122* (28), 6759-6764.
15. Chakraborty, S.; Raj, C. R. Mediated electrocatalytic oxidation of bioanalytes and biosensing of glutamate using functionalized multiwall carbon nanotubes-biopolymer nanocomposite. *Journal of Electroanalytical Chemistry* **2007**, *609* (2), 155-162.
16. Nagaoka, T.; Sakai, T.; Ogura, K.; Yoshino, T. Oxygen reduction at electrochemically treated glassy carbon electrodes. *Analytical Chemistry* **1986**, *58* (9), 1953-1955.
17. Zhang, J.; Wang, X.; Su, Q.; Zhi, L.; Thomas, A.; Feng, X.; Su, D. S.; Schlögl, R.; Müllen, K. Metal-free phenanthrenequinone cyclotrimer as an effective heterogeneous catalyst. *Journal of the American Chemical Society* **2009**, *131* (32), 11296-11297.
18. Li, X.; Liu, T.; Liu, L.; Li, F. Dependence of the electron transfer capacity on the kinetics of quinone-mediated Fe (III) reduction by two iron/humic reducing bacteria. *RSC Advances* **2014**, *4* (5), 2284-2290.
19. Li, X.; Liu, L.; Liu, T.; Yuan, T.; Zhang, W.; Li, F.; Zhou, S.; Li, Y. Electron transfer capacity dependence of quinone-mediated Fe (III) reduction and current generation by *Klebsiella pneumoniae* L17. *Chemosphere* **2013**, *92* (2), 218-224.

20. Burgos, W. D.; Fang, Y.; Royer, R. A.; Yeh, G.-T.; Stone, J. J.; Jeon, B.-H.; Dempsey, B. A. Reaction-based modeling of quinone-mediated bacterial iron (III) reduction. *Geochimica et cosmochimica acta* **2003**, *67* (15), 2735-2748.
21. Wu, Y.; Li, F.; Liu, T.; Han, R.; Luo, X. pH dependence of quinone-mediated extracellular electron transfer in a bioelectrochemical system. *Electrochimica Acta* **2016**, *213*, 408-415.
22. Petek, T. J.; Hoyt, N. C.; Savinell, R. F.; Wainright, J. S. Slurry electrodes for iron plating in an all-iron flow battery. *Journal of Power Sources* **2015**, *294*, 620-626.
23. Wei, L.; Wu, M. C.; Zhao, T. S.; Zeng, Y. K.; Ren, Y. X. An aqueous alkaline battery consisting of inexpensive all-iron redox chemistries for large-scale energy storage. *Applied Energy* **2018**, *215*, 98-105.
24. Li, D.; Batchelor-McAuley, C.; Compton, R. G. Some thoughts about reporting the electrocatalytic performance of nanomaterials. *Applied Materials Today* **2019**.
25. Guidelli, R.; Compton, R. G.; Feliu, J. M.; Gileadi, E.; Lipkowski, J.; Schmickler, W.; Trasatti, S. Definition of the transfer coefficient in electrochemistry (IUPAC Recommendations 2014). *Pure and Applied Chemistry* **2014**, *86* (2), 259-262.
26. Guidelli, R.; Compton, R. G.; Feliu, J. M.; Gileadi, E.; Lipkowski, J.; Schmickler, W.; Trasatti, S. Defining the transfer coefficient in electrochemistry: An assessment (IUPAC Technical Report). *Pure and Applied Chemistry* **2014**, *86* (2), 245-258.
27. Gileadi, E. Problems in interfacial electrochemistry that have been swept under the carpet. *Journal of Solid State Electrochemistry* **2011**, *15* (7-8), 1359.
28. Thorogood, C. A.; Wildgoose, G. G.; Crossley, A.; Jacobs, R. M. J.; Jones, J. H.; Compton, R. G. Differentiating between ortho-and para-quinone surface groups on graphite, glassy carbon, and carbon nanotubes using organic and inorganic voltammetric and X-ray photoelectron spectroscopy labels. *Chemistry of Materials* **2007**, *19* (20), 4964-4974.
29. Harrington, M. J.; Masic, A.; Holten-Andersen, N.; Waite, J. H.; Fratzl, P. Iron-clad fibers: a metal-based biological strategy for hard flexible coatings. *Science* **2010**, *328* (5975), 216-220.
30. Holten-Andersen, N.; Harrington, M. J.; Birkedal, H.; Lee, B. P.; Messersmith, P. B.; Lee, K. Y. C.; Waite, J. H. pH-induced metal-ligand cross-links inspired by mussel yield self-healing polymer networks with near-covalent elastic moduli. *Proceedings of the National Academy of Sciences* **2011**, *108* (7), 2651-2655.
31. Sato, K.; Ohsaka, T.; Matsuda, H.; Oyama, N. Electrocatalytic Reaction of Fe<sup>2+</sup>/3+ Aqua Ions by [Mo (CN) <sub>8</sub>] <sup>4-</sup>/3- Complexes. *Bulletin of the Chemical Society of Japan* **1983**, *56* (6), 1863-1864.